JACS
JOURNAL OF THE AMERICAN CHEMICAL SOCIETY

COMMUNICATION

pubs.acs.org/JACS

Making the Golden Connection: Reversible Mechanochemical and Vapochemical Switching of Luminescence from Bimetallic Gold–Silver Clusters Associated through Aurophilic Interactions

Tania Lasanta,[†] M. Elena Olmos,[†] Antonio Laguna,[‡] José M. López-de-Luzuriaga,*[,†] and Panče Naumov*[,§]

[†]Departamento de Química, Universidad de la Rioja, Grupo de Síntesis Química de La Rioja, UA-CSIC Complejo Científico Tecnológico, E-26001 Logroño, Spain

[‡]Departamento de Química Inorgánica-ISQCH, Universidad de Zaragoza-CSIC, E-50009 Zaragoza, Spain

[§]Department of Material and Life Science, Graduate School of Engineering, Osaka University, 2-1 Yamada-oka, 565-0871 Suita, Osaka, Japan

Supporting Information

ABSTRACT: Aiming at the development of new architectures within the context of the quest for strongly luminescent materials with tunable emission, we utilized the propensity of the robust bimetallic clusters $[Au_2Ag_2(R^I/R^{II})_4]$ (R^I = 4-C_6F_4I, R^{II} = 2-C_6F_4I) for self-assembly through aurophilic interactions. With a de novo approach that combines the coordination and halogen-bonding potential of aromatic heteroperhalogenated ligands, we have generated a family of remarkably luminescent bimetallic materials that provide grounds to address the relevance, relative effects, and synergistic action of the two interactions in the underlying photophysics. By polymerizing the green-emitting (λ^{em}_{max} = 540 nm) *monomer* $[Au_2Ag_2R^{II}_4(tfa)_2]^{2-}$ (tfa = trifluoroacetate) to a red-emitting (λ^{em}_{max} = 660 nm) *polymer* $[Au_2Ag_2R^{II}_4(MeCN)_2]_n$, we demonstrate herein that the degree of cluster association in these materials can be effectively and reversibly switched simply by applying mechanochemical and/or vapochemical stimuli in the solid state as well as by solvatochemistry in solution, the reactions being coincident with a dramatic switching of the intense, readily perceptible photoluminescence. We demonstrate that the key event in the related equilibrium is the evolution of a metastable yellow emitter (λ^{em}_{max} = 580 nm) for which the structure determination in the case of the ligand R^{II} revealed a *dimeric* nonsolvated topology $[Au_2Ag_2R^{II}_4]_2$. Taken together, these results reveal a two-stage scenario for the aurophilic-driven self-assembly of the bimetallic clusters $[Au_2Ag_2(R^I/R^{II})_4]$: (1) initial association of the green-emitting monomers to form metastable yellow-emitting dimers and desolvation followed by (2) resolvation of the dimers and their self-assembly to form a red-emitting linear architecture with delocalized frontier orbitals and a reduced energy gap. The green emission from $[Au_2Ag_2R^{II}_4(tfa)_2]^{2-}$ (λ^{em}_{max} = 540 nm) exceeds the highest energy observed for $[Au_2Ag_2]$-based structures to date, thereby expanding the spectral slice for emission from related structures beyond 140 nm, from the green region to the deep-red region.

Metal–organic architectures based on aurophilic interactions (AIs)[1] and, more generally, on metallophilic interactions (MIs), typically between gold(I) and closed-shell metal centers[2] such as silver(I)[3](Scheme 1), present a remarkably rich and exciting solution- and solid-state coordination chemistry while exhibiting an impressive panoply of tunable photoluminescent, piezochromic, and vapochromic properties that are of relevance for applications in luminescence signaling and vapochemical sensing,[4] among others. The Au···Ag MIs in these heteropolynuclear cluster-type structures can be conveniently accessed by an acid–base methodology that utilizes a combination of the anionic bis(perfluorophenyl)aurate unit $Au(C_6F_5)_2^-$ and silver(I)-based Lewis acids to self-assemble the robust building block $[Au_2Ag_2(C_6F_5)_4]$.[5] We have recently added to the supramolecular complexity of these architectures by replacing the $[Au_2Ag_2(C_6F_5)_4]$ unit with its heteroperhalophenyl analogue $[Au_2Ag_2(4\text{-}C_6F_4I)_4]$.[6] The rationale behind the utility of 4-C_6F_4I stems from the excellent Lewis acidity of the strongly polarized *p*-iodine atom and its propensity to form strong halogen bonds (XBs),[7] interactions that are now being increasingly recognized for their critical relevance in the structure–property profiles of halogen-containing systems that are devoid of stronger directional intermolecular interactions.[8] The emission energy of the resulting polymeric argentoaurophilic clusters indicates an intricate synergy between the AIs and XBs in the control of the emission energy, the two interactions apparently affecting the excited-state profile through different frontier orbitals.[6,9]

Intrigued by the possibility of exercising concerted control over the strong photoluminescence observed with these systems

Scheme 1. Structures of the Perhalogenated Ligands R^I and R^{II} and Bonding Motifs Conjectured on the Basis of the Combined Action of Aurophilic Interactions (AIs), Metallophilic Interactions (MIs), and Halogen Bonds (XBs)

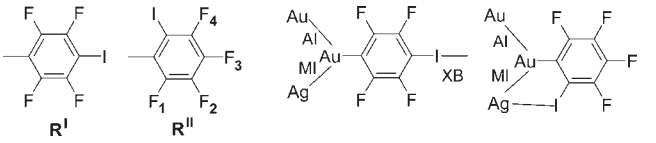

Received: July 21, 2011
Published: September 12, 2011

dx.doi.org/10.1021/ja206845s | *J. Am. Chem. Soc.* 2011, 133, 16358–16361

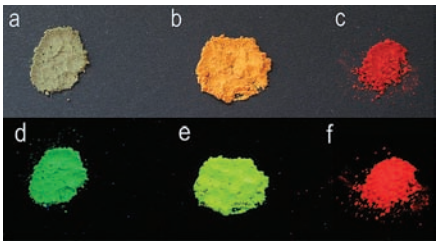

Figure 1. (a–c) Appearance of **1**, **2**, and **3** under visible light and (d–f) luminescence of **1**, **2**, and **3** induced by exposure to weak UV light from a mercury lamp.

by means of reversible solvent coordination and mechanical shear, we embarked on designing new topologies by purposeful alteration of the availability of the Au(I) and Ag(I) centers for AIs *and* of the polarized iodine atom for XBs. The intention of the present work was to examine whether both goals could be achieved concurrently by substituting the phenyl group in the central structural motif $[Au_2Ag_2(C_6H_5)_4]$ with 2-C_6F_4I (R^I) or 4-C_6F_4I (R^{II}). Indeed, the iodine in 2-C_6F_4I is less polarized and points away from the potential XB acceptors, and thus it is less available for XBs relative to 4-C_6F_4I. By bidentate coordination to Ag(I), it can contribute to partial saturation of the coordination capacity of the bimetallic clusters and mitigation of their propensity for polymerization. The new materials prepared following this strategy exhibit remarkable mechanochromic and vapochromic properties and are strongly photoluminescent. Moreover, we observed a dynamic coordination equilibrium between the structures with different emission that can be controlled both vapochemically and mechanochemically in the solid state as well as in solution. With one of these structures, we succeeded in shifting the high-energy limit of the emission wavelength deeper into the green region, beyond the shortest wavelength that has been reported to date for related structures. The collection of bimetallic structures currently covers a 140 nm slice of the energy spectrum, and their emission color can be tuned from green through yellow, orange, and red to deep-red. Taken together, these results corroborate the critical role of the AIs in tuning the strong photoluminescence and hint at a new strategy for shifting the emission toward the blue region.

The synthesis of the intermetallic Au_2Ag_2 clusters was achieved by reacting Ag(tfa) (tfa = trifluoroacetate) in CH_2Cl_2 with an equimolar amount of $NBu_4[Au(2\text{-}C_6F_4I)_2]$[9] [for synthesis and characterization details, see the Supporting Information (SI)]. A product having the stoichiometry $(NBu_4)_2[Au_2Ag_2(2\text{-}C_6F_4I)_4(tfa)_2]$ (**1**) was obtained as a beige-to-gray solid with *green* luminescence (λ^{em}_{max} = 540 nm; Figure 1a,d). The presence of the tfa ion was corroborated in the ^{19}F NMR spectrum (acetone-d_6) by a singlet at −73.0 ppm and peaks corresponding to four types of nonequivalent fluorine atoms: −113.8 (m, 4F, F_4), −114.2 (m, 4F, F_1), −157.6 (m, 4F, F_2) and −160.0 ppm (m, 4F, F_3). The molar conductivity of **1** in acetone confirmed the ionic nature proposed by its stoichiometry. Addition of a few drops of a coordinating solvent such as MeCN to the powder of **1** triggered a gradual and drastic change in the emission color from green to yellow to orange-red (Figure 2a–f), indicative of the formation of a solvated product, **3**. The presence of MeCN was confirmed by IR bands at 2297 and 2264 cm^{-1}, corresponding to the MeCN stretching (C≡N) mode, and a singlet at 2.17 ppm in the ^{1}H NMR spectrum ($CDCl_3$), showing dissociation of the coordinated solvent in solution. The ^{19}F NMR spectrum of **3**, recorded

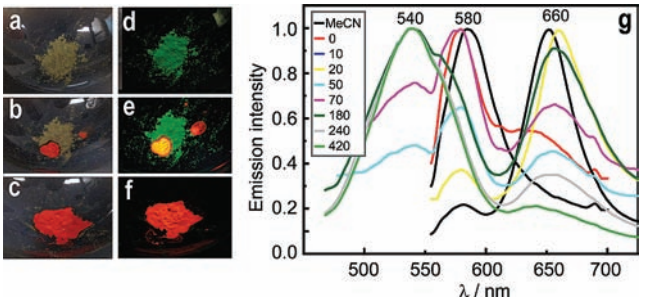

Figure 2. (a–f) Changes in (a–c) color and (d–f) luminescence induced by addition of MeCN to **1** in the solid state. Panels b and e show the sample immediately after addition of a drop of MeCN (note the spot with a bright-yellow emission), and panels c and f show its appearance after standing. (g) Monitoring of the solvent-induced reaction and subsequent aging-induced desolvation of **1** by reflectance emission spectroscopy. The values topping the peaks correspond to the emission maxima (in nm), and the numbers in the box correspond to the time (in minutes) lapsed after the addition of MeCN.

in its own deuterated solvent because of its low solubility in chlorinated solvents, was typical for Au(I)-coordinated 2-C_6F_4I.

Monitoring of the time course of solvation of solid **1** with MeCN by reflectance emission spectroscopy (Figure 2g) showed that the strong luminescence at 540 nm was initially replaced by a yellow emission at λ^{em}_{max} = 580 nm. In less than 10 min, the new band at 580 nm was gradually replaced with another one at λ^{em}_{max} = 660 nm, corresponding to the strong red luminescence from the solvated product **3** (Figure 1c,f). When the product **3** obtained by addition of MeCN to **1** was kept at ambient temperature, slow and spontaneous desolvation occurred, stimulating the reverse series of events. The intensity of the 660 nm band decreased with a concomitant increase in the intensity of the 580 nm band. After 30 min, the intensity of the 540 nm band of **1** was also visibly recovered, and within 1 h after the solvent addition, all three species coexisted. After aging for less than 7 h, the 540 nm emission of **1** was completely recovered (Figure 2g). We found that grinding in the presence of tfa had a strong effect on the reverse transformation. Indeed, gentle grinding of solid **3** with powdered NBu_4(tfa) resulted in rapid and complete recovery of the green luminescence of **1** in several minutes.

Single crystals of the green-emitting material **1** suitable for X-ray diffraction (XRD) were obtained by slow diffusion of Et_2O into a solution of the product in a noncoordinating solvent (CH_2Cl_2). The structure is composed of tetranuclear *monomers* (two independent molecules in the asymmetric unit), and the Au–Ag MI distances within the tetranuclear units range from 2.7738(7) to 2.9269(7) Å. Each of the Au(I) atoms is linearly coordinated by two 2-C_6F_4I groups, and each Ag(I) is O-coordinated by tfa ion [2.524(6)–2.645(11) Å] (Figure 3). As expected from the strong Lewis acidity of Ag(I) and the *ortho* disposition of the iodine atom, stabilization of the structure by coordination outweighs the affinity for XBs, so in the $[Au_2Ag_2(2\text{-}C_6F_4I)_4(tfa)_2]^{2-}$ clusters, both 2-C_6F_4I ligands on each Au(I) are coordinated to the Ag(I) ions, with Ag–I distances of 2.7987(9)–2.9011(9) Å.

The red-emitting **3** was prepared in the pure state by reacting solid **1** with MeCN and also by addition of MeCN to a solution of **1** prepared in situ from $NBu_4[Au(2\text{-}C_6F_4I)_2]$ and $AgClO_4$ in 2:1 CH_2Cl_2/Et_2O; the two methods afforded identical products. **3** was isolated as a red solid with vivid *red* luminescence (Figure 1c,f)

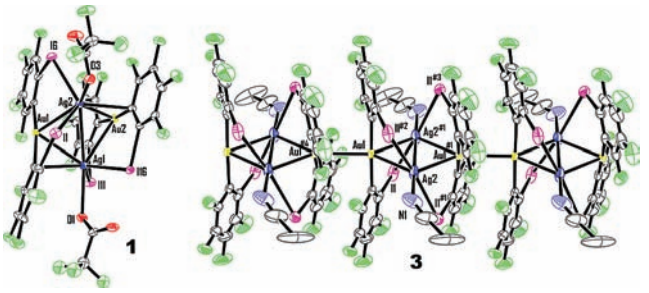

Figure 3. ORTEP-style diagrams (30% probability level) of (left) the cluster in $(NBu_4)_2[Au_2Ag_2(2\text{-}C_6F_4I)_4(tfa)_2]$ (**1**) and (right) a portion of the infinite-cluster polymers in $[Au_2Ag_2(2\text{-}C_6F_4I)_4(MeCN)_2]_n$ (**3**). The methyl hydrogen atoms in the structure of **3** have been omitted for clarity. Symmetry codes: #1: $1.5 - x$; $0.5 - y$, z. #2: x, $0.5 - y$, $1.5 - z$; #3: $1.5 - x$, y, $1.5 - z$; #4: $x - 0.5$, y, z.

identical to that observed for the product of solvation of solid **1** with MeCN (Figure 2c,f). Single crystals of **3** suitable for XRD studies were grown by diffusion of Et_2O in a MeCN solution of **1**. The XRD analysis revealed a *polymeric* linear structure in which both tfa ligands are replaced with solvent molecules (Figure 3). Through Au···Au AIs [3.0212(8) Å], the $[Au_2Ag_2(2\text{-}C_6F_4I)_4]$ blocks in **3** are self-assembled into infinite $[Au_2Ag_2(2\text{-}C_6F_4I)_4(MeCN)_2]_n$ linear chains. As in **1**, the $2\text{-}C_6F_4I$ groups act as bridging ligands: the two $2\text{-}C_6F_4I$ ligands from the two Au(I) atoms are coordinated to different Ag(I) atoms.

The time profile of the solid-state emission spectra and the absence of an isosbestic point in Figure 2g indicate that the conversion between the green-emitting monomeric clusters in **1** and the red-emitting polymers in **3**, which can be induced by exposure to solvents, aging, or grinding, proceeds through a yellow-emitting intermediate, **2**, whose structure can provide valuable insight into the mechanism of the formation of AIs. Repeated attempts to crystallize the yellow-emitting material starting from **1** and MeCN or from **3** and $NBu_4(tfa)$ were unsuccessful. However, when $NBu_4(tfa)$ used for grinding of **3** was replaced with NBu_4ClO_4, a powder product that emitted bright-yellow light was obtained (Figure 4), hinting that removal of tfa from the system terminated the conversion of **3** to **1** at the intermediate stage **2**. Indeed, by reaction of equimolar amounts of $NBu_4[Au(2\text{-}C_6F_4I)_2]$ and $AgClO_4$ in 2:1 CH_2Cl_2/Et_2O and diffusion of *n*-hexane into a solution of the product in THF, we obtained yellow-luminescent crystals whose analytical data (see the SI) conformed to those of the powder of **2** and the stoichiometry $[Au_2Ag_2(2\text{-}C_6F_4I)_4]_2\cdot 4NBu_4ClO_4\cdot THF$.[10] The MALDI−TOF spectrum displays a peak at m/z 1600 (100% $[Au_2Ag(2\text{-}C_6F_4I)_4]^-$). The IR spectrum shows the $(2\text{-}C_6F_4I)^-$ absorptions at 1607, 1589, 1081, and 811 cm^{-1} due to the vibrations of the coordinated $2\text{-}C_6F_4I$ ligands. Solid **2** is selectively vapochromic toward coordinating solvents: brief exposure to acetone, THF, or MeCN vapors resulted in rapid color change. The solvated products, for which the analytical data showed the composition $[Au_2Ag_2(2\text{-}C_6F_4I)_4L_2]_n$ [L = Me_2CO (**4**), THF (**5**)], were obtained as pure phases by recrystallization from the respective solvents, as described above for **3** (for details, see the SI), thus authenticating that the Ag(I) ions in **2** are coordinatively unsaturated.

The crystal structure determination of $\mathbf{2}\cdot 4NBu_4ClO_4\cdot THF$ (Figure 5) unraveled three rather unanticipated but very important features: (1) the $[Au_2Ag_2(2\text{-}C_6F_4I)_4]$ clusters are *dimerized*;

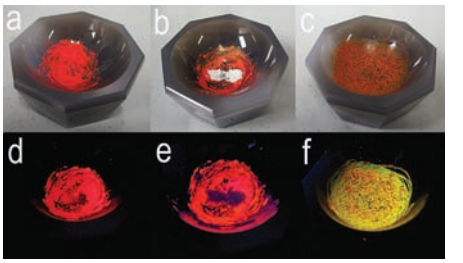

Figure 4. (a−c) Color and (d−f) luminescence of $[Au_2Ag_2(2\text{-}C_6F_4I)_4(MeCN)_2]_n$ (**3**) (a, d) after grinding in the pure state, (b, e) after addition of NBu_4ClO_4, and (c, f) after grinding of the mixture.

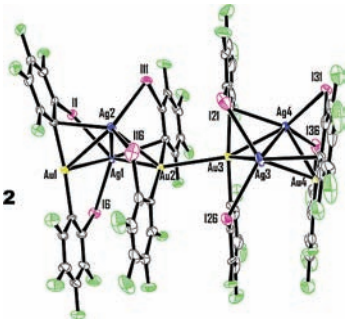

Figure 5. ORTEP-style diagram (30% probability level) of the dimer of bimetallic clusters in the crystal structure of $[Au_2Ag_2(2\text{-}C_6F_4I)_4]_2\cdot 4NBu_4ClO_4\cdot THF$ ($\mathbf{2}\cdot 4NBu_4ClO_4\cdot THF$).

Scheme 2. Schematic Representation of the Chemical Equilibrium among 1, 2, and 3

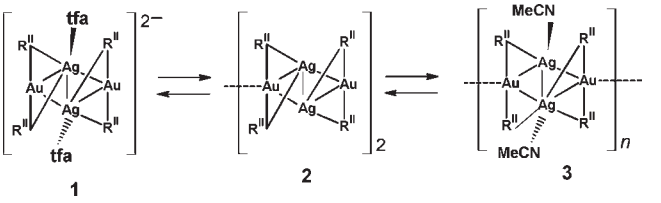

(2) despite the presence of THF molecules in the lattice, the Ag(I) centers are devoid of organic ligands; and (3) the transformation of **1** into **3** is associated with flattening of the tetranuclear Au_2Ag_2 clusters, as reflected in the angles between the $AuAg_2$ planes (112° in **1**, 118° in $\mathbf{2}\cdot 4NBu_4ClO_4\cdot THF$, and 180° in **3**).

The spectral−structural profile of **1**−**3** can be now rationalized by depicting the reaction scenario for self-assembly of the $[Au_2Ag_2(2\text{-}C_6F_4I)_4]$ clusters, wherein **1** and **3** represent the terminal stages while **2** is the intermediate stage of that process (Scheme 2). According to this picture, addition of MeCN to **1** in the solid state or in solution initially induces dimerization and removal of the tfa ligands. MeCN then coordinates to the dimers, which polymerize through Au···Au interactions to give the linear chains of **3**. The equilibrium between **1** and **3** can be shifted through **2** in either direction by adding or removing MeCN or tfa. The extent of polymerization (**1** < **2** ≪ **3**) is clearly reflected in the corresponding emission wavelengths (540 nm < 580 nm < 660 nm), evidencing that the expansion of the clusters causes a

dx.doi.org/10.1021/ja206845s |*J. Am. Chem. Soc.* 2011, 133, 16358–16361

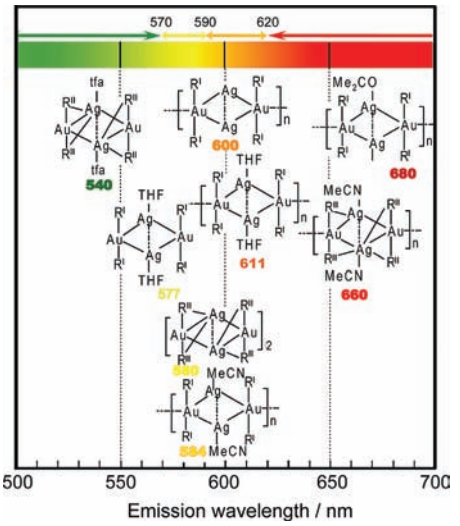

Figure 6. Summary of the structures and luminescence energies of the bimetallic Au−Ag complexes with aryl ligands (R^I = 4-C_6F_4I, R^{II} = 2-C_6F_4I).

red shift of the emission. The first stage (dimerization) causes a red shift of 40 nm, while the subsequent extension of the polymer to infinity causes a red shift of only 80 nm. This observation emphasizes the limited effect on the emission by delocalization of the relevant orbitals determining the excited-state energy. A noteworthy observation here is that the emission maximum of the green-emitting **1**, 540 nm, is the shortest wavelength among the related structures. As the longest wavelength (680 nm) was reported for $[Au_2Ag_2(4\text{-}C_6F_4I)_4(MeCN)_2]_n$,[6] the bimetallic cluster structures with perhalogenated phenyl ligands, $[Au_2Ag_2(R^I/R^{II})_4]$ (R^I = 4-C_6F_4I, R^{II} = 2-C_6F_4I), cover a 140 nm slice of the visible spectrum (Figure 6). The results conspicuously demonstrate that by changing the potency of the ligand for AIs and XBs, the emission color can be tuned from green through yellow, orange, and red to deep-red. These results corroborate the critical role of the AIs and XBs in tuning the strong photoluminescence. They also hint at using negatively charged intermetallic assemblies as a new and alternative strategy for shifting the emission into the blue region as well as pave the way for future applications of these materials as multicolor sensors.

■ ASSOCIATED CONTENT

Supporting Information. Experimental details and crystallographic data (CIF). This material is available free of charge via the Internet at http://pubs.acs.org.

■ AUTHOR INFORMATION

Corresponding Author
josemaria.lopez@unirioja.es; pancenaumov@gmail.com

■ ACKNOWLEDGMENT

This work was supported by Project D.G.I.(MEC)/FEDER (CTQ2010-20500-C02-02) and partially also by a Global COE Program, "The Global Education and Research Center for Bio-Environmental Chemistry", from the Ministry of Education, Culture, Sports, Science and Technology, Japan. T.L. thanks MICINN for a grant.

■ REFERENCES

(1) (a) Schmidbaur, H. *Chem. Soc. Rev.* **2008**, *37*, 1931. (b) Pyykkö, P. *Angew. Chem., Int. Ed.* **2004**, *43*, 4412. (c) Schmidbaur, H.; Graf, W.; Müller, G. *Angew. Chem., Int. Ed. Engl.* **1991**, *30*, 604. (d) *Gold: Progress in Chemistry, Biochemistry and Technology*; Schmidbaur, H., Ed.; Wiley: New York, 1999. (e) Schmidbaur, H. *Nature* **2001**, *413*, 31. (f) Schmidbaur, H. *Gold Bull.* **1990**, *23*, 11.

(2) (a) Carlson, T. F.; Fackler, J. P., Jr.; Staples, R. J.; Winpenny, R. E. P. *Inorg. Chem.* **1995**, *34*, 426. (b) Crespo, O.; Laguna, A.; Fernández, E. J.; López-de-Luzuriaga, J. M.; Jones, P. G.; Teichert, M.; Monge, M.; Pyykkö, P.; Runeberg, N.; Schütz, M.; Werner, H. J. *Inorg. Chem.* **2000**, *39*, 4786. (c) Bardají, M.; Laguna, A. *Eur. J. Inorg. Chem.* **2003**, 3069. (d) Catalano, V. J.; Bennett, B. L.; Malwitz, M. A.; Yson, R. L.; Kar, H. M.; Muratidis, S.; Horner, S. J. *Comments Inorg. Chem.* **2003**, *24*, 39.

(3) (a) Rawashdeh-Omary, M. A.; Omary, M. A.; Fackler, J. P., Jr. *Inorg. Chim. Acta* **2002**, *334*, 376. (b) Crespo, O.; Fernández, E. J.; Gil, M.; Gimeno, M. C.; Jones, P. G.; Laguna, A.; López-de-Luzuriaga, J. M.; Olmos, M. E. *J. Chem. Soc., Dalton Trans.* **2002**, 1319. (c) Catalano, V. J.; Horner, S. J. *Inorg. Chem.* **2003**, *42*, 8430. (d) Catalano, V. J.; Malwitz, M. A.; Etogo, A. O. *Inorg. Chem.* **2004**, *43*, 5714. (e) Römbke, P.; Schier, A.; Schmidbaur, H.; Cronje, S.; Raubenheimer, H. *Inorg. Chim. Acta* **2004**, *357*, 235.

(4) (a) Fernández, E. J.; López-de-Luzuriaga, J. M.; Monge, M.; Olmos, M. E.; Pérez, J.; Laguna, A.; Mohammed, A. A.; Fackler, J. P., Jr. *J. Am. Chem. Soc.* **2003**, *125*, 2022. (b) Fiddler, M. N.; Begashaw, L.; Mickens, M. A.; Collingwood, M. S.; Assefa, Z.; Bililign, S. *Sensors* **2009**, *9*, 10447. (c) Elosúa, C.; Bariain, C.; Matias, I. R.; Arregui, F. J.; Vergara, E.; Laguna, M. *Sens. Actuators, B* **2009**, *137*, 139. (d) Lim, A. H.; Olmstead, M. M.; Balch, A. L. *J. Am. Chem. Soc.* **2011**, *133*, 10229. (e) Ito, H.; Saito, T.; Oshima, N.; Kitamura, N.; Ishizaka, S.; Hinatsu, Y.; Wakeshima, M.; Kato, M.; Tsuge, K.; Sawamura, M. *J. Am. Chem. Soc.* **2008**, *130*, 10044.

(5) (a) Fernández, E. J.; Gimeno, M. C.; Laguna, A.; López-de-Luzuriaga, J. M.; Monge, M.; Pyykkö, P.; Sundholm, D. *J. Am. Chem. Soc.* **2000**, *122*, 7287. (b) Fernández, E. J.; Laguna, A.; López-de-Luzuriaga, J. M.; Montiel, M.; Olmos, M. E.; Pérez, J.; Puelles, R. C. *Organometallics* **2006**, *25*, 4307. (c) Fernández, E. J.; Jones, P. G.; Laguna, A.; López-de-Luzuriaga, J. M.; Monge, M.; Olmos, M. E.; Puelles, R. C. *Organometallics* **2007**, *26*, 5931. (d) López-de-Luzuriaga, J. M. Luminescence of Supramolecular Gold-Containing Materials. In *Modern Supramolecular Gold Chemistry: Gold−Metal Interactions and Applications*; Laguna, A., Ed.; Wiley-VCH: Weinheim, Germany, 2008; pp 347 ff.

(6) Laguna, A.; Lasanta, T.; López-de-Luzuriaga, J. M.; Monge, M.; Naumov, P.; Olmos, M. E. *J. Am. Chem. Soc.* **2010**, *132*, 456.

(7) (a) Metrangolo, P.; Neukirch, H.; Pilati, T.; Resnati, G. *Acc. Chem. Res.* **2005**, *38*, 386. (b) Cabot, R.; Hunter, C. A. *Chem. Commun.* **2009**, 2005.

(8) Selected examples: (a) Metrangolo, P.; Carcenac, Y.; Lahtinen, M.; Pilati, T.; Rissanen, K.; Vij, A.; Resnati, G. *Science* **2009**, *323*, 1461. (b) Assefa, Z.; Omary, M. A.; McBurnett, B. G.; Mohamed, A. A.; Patterson, H. H.; Staples, R. J.; Fackler, J. P., Jr. *Inorg. Chem.* **2002**, *41*, 6274. (c) Lee, Y. A.; Eisenberg, R. *J. Am. Chem. Soc.* **2003**, *125*, 7778. (d) Walsh, R. B.; Padgett, C. W.; Metrangolo, P.; Resnati, G.; Hanks, T. W.; Pennington, W. T. *Cryst. Growth Des.* **2001**, *1*, 165. (e) Mínguez Espallargas, G.; Brammer, L.; Allan, D. R.; Pulham, C. R.; Robertson, N.; Warren, J. E. *J. Am. Chem. Soc.* **2008**, *130*, 9058. (f) Libri, S.; Jasim, N. A.; Perutz, R. N.; Brammer, L. *J. Am. Chem. Soc.* **2008**, *130*, 7842. (g) Amati, M.; Lelj, F.; Liantonio, R.; Metrangolo, P.; Luzzati, S.; Pilati, T.; Resnati, G. *J. Fluorine Chem.* **2004**, *125*, 629.

(9) Fernández, E. J.; Laguna, A.; Lasanta, T.; López-de-Luzuriaga, J. M.; Montiel, M.; Olmos, M. E. *Organometallics* **2008**, *27*, 2971.

(10) The ^{19}F NMR spectrum could not be recorded because of insolubility in chlorinated solvents.